NIH Public Access
Author Manuscript
JACC Cardiovasc Imaging. Author manuscript; available in PMC 2010 May 12.

Published in final edited form as:
JACC Cardiovasc Imaging. 2008 May ; 1(3): 354–362. doi:10.1016/j.jcmg.2007.11.007.

Noninvasive Imaging of Angiotensin Receptors After Myocardial Infarction

Johan W. H. Verjans, MD[*,‖], **Dagfinn Lovhaug, PhD**[§], **Navneet Narula, MD**[†], **Artiom D. Petrov, PhD**[*], **Bård Indrevoll, MS**[§], **Emma Bjurgert, PhD**[§], **Tatiana B. Krasieva, PhD**[‡], **Lizette B. Petersen, MS**[§], **Grete M. Kindberg, PhD**[§], **Magne Solbakken, PhD**[§], **Alan Cuthbertson, PhD**[§], **Mani A. Vannan, MD, FACC**[*], **Chris P. M. Reutelingsperger, PhD**[‖], **Bruce J. Tromberg, PhD**[‡], **Leonard Hofstra, MD, PhD**[‖], and **Jagat Narula, MD, PhD, FACC**[*]

[*]Department of Cardiology, University of California at Irvine, Irvine, California [†]Department of Pathology, University of California at Irvine, Irvine, California [‡]Beckman Laser Institute, University of California at Irvine, Irvine, California [§]GE Healthcare, Oslo, Norway [‖]Cardiovascular Research Institute, Maastricht University, Maastricht, the Netherlands.

Abstract

OBJECTIVES—The purpose of this study was to evaluate the feasibility of noninvasive imaging of angiotensin II (AT) receptor upregulation in a mouse model of post-myocardial infarction (MI) heart failure (HF).

BACKGROUND—Circulating AT levels do not reflect the status of upregulation of renin-angiotensin axis in the myocardium, which plays a central role in ventricular remodeling and evolution of HF after MI. Appropriately labeled AT or AT receptor blocking agents should be able to specifically target AT receptors by molecular imaging techniques.

METHODS—AT receptor imaging was performed in 29 mice at various time points after permanent coronary artery ligation or in controls using a fluoresceinated angiotensin peptide analog (APA) and radiolabeled losartan. The APA was used in 19 animals for intravital fluorescence microscopy on a beating mouse heart. Tc-99m losartan was used for in vivo radionuclide imaging and quantitative assessment of AT receptor expression in 10 mice. After imaging, hearts were harvested for pathological characterization using confocal and 2-photon microscopy.

RESULTS—No or little APA uptake was observed in control animals or within infarct regions on days 0 and 1. Distinct uptake occurred in the infarct area at 1 to 12 weeks after MI; the uptake was at maximum at 3 weeks and reduced markedly at 12 weeks after MI. Ultrasonographic examination demonstrated left ventricular remodeling, and pathologic characterization revealed localization of the APA tracer with collagen-producing myofibroblasts. Tc-99m losartan uptake in the infarct region (0.524 ± 0.212% injected dose/g) increased 2.4-fold as compared to uptake in the control animals (0.215 ± 0.129%; $p < 0.05$).

CONCLUSIONS—The present study demonstrates the feasibility of in vivo molecular imaging of AT receptors in the remodeling myocardium. Noninvasive imaging studies aimed at AT receptor expression could play a role in identification of subjects likely to develop heart failure. In addition, such a strategy could allow for optimization of anti-angiotensin therapy in patients after MI.

© 2008 BY THE AMERICAN COLLEGE OF CARDIOLOGY FOUNDATION PUBLISHED BY ELSEVIER INC.

Reprint requests and correspondence: Dr. Jagat Narula OR Dr. Leo Hofstra, University of California, Irvine, School of Medicine, 101 The City Drive, Bldg. 53, Mail Route 81, Orange, California 92868-4080. narula@uci.edu *OR* l.hofstra@cardio.unimaas.nl..

NIH-PA Author Manuscript
NIH-PA Author Manuscript
NIH-PA Author Manuscript

NIH-PA Author Manuscript

NIH-PA Author Manuscript

NIH-PA Author Manuscript

It is well established that myocardial, more so than the systemic neurohumoral upregulation, contributes to ventricular remodeling and development of heart failure (HF) after myocardial infarction (MI) (1). In particular, myocardial angiotensin II (AT) type-1 receptor expression is associated with interstitial fibrosis and ventricular dysfunction (2). Transgenic mice with deficient AT type-1 receptor expression exhibit minimal geometric and structural remodeling following MI, and show lesser upregulation of fetal genes, transforming growth factor beta-1, and collagen deposition in comparison with the wild-type animals (3). Clinical use of angiotensin-converting enzyme (ACE) inhibitors and angiotensin receptor blockers in MI retards ventricular remodeling, delays development of HF, reduces rehospitalization for worsening of HF, and improves survival (4–8).

Because myocardial neurohumoral upregulation is associated with ventricular remodeling, we hypothesized that a novel diagnostic strategy targeted at detecting the extent of myocardial AT receptor expression would allow identification of patients at risk of developing HF. In addition, such a strategy should allow optimization of pharmacologic therapy in HF patients. Because subcellular processes are amenable to noninvasive molecular imaging techniques, we labeled an angiotensin peptide analog (APA) with a fluorescent tracer. The APA targeted both angiotensin type-1 and -2 receptors with high affinity (K_i = 3 pmol/l), and optical imaging was performed to determine the myocardial upregulation of AT receptors after MI in an experimental mouse model. To more specifically target AT type-1 receptors, we also radiolabeled losartan, a commonly used AT type-1 receptor blocker, and performed imaging with micro–single-photon emission computed tomograpy and micro-computed tomography.

METHODS

The present study was performed in 29 mice (Table 1). Of these, 19 mice were studied with fluorescent APA; 16 mice were imaged up to 12 weeks after MI and compared with 3 noninfarcted control animals. For radionuclide imaging, technetium-99m (^{99m}Tc) losartan was used in 4 mice 3 weeks after MI and 6 noninfarcted control animals (Table 1). Echocardiography was performed for the assessment of left ventricular (LV) dimensions and function in all mice prior to optical imaging. Optical imaging was performed in open chest preparation. Noninvasive radionuclide imaging was performed on mice by micro-single-photon emission computed tomography (SPECT)/micro-computed tomography (CT) coregistration. All animals were sacrificed after optical or nuclear imaging. The myocardial specimens from animals receiving the fluorescent tracer were characterized histologically by localizing the injected probe with confocal and 2-photon microscopy in frozen samples as well as by hematoxylin and eosin staining of paraffinembedded tissue. Myocardial specimens obtained from animals after nuclear imaging were used to determine quantitative uptake of radiolabeled losartan in the myocardium. All experiments were approved by the Institutional Animal Care and Use Committee at the University of California, Irvine and were conducted in accordance with U.S. guidelines on the humane care and use of research animals.

Synthesis of fluorescein APA for optical imaging

The peptidyl resin H-Arg(Pmc)-Val-Tyr(tBu)-Ile-His(Trt)-Pro-Ile-R was synthesized on an Applied Biosystems 433A peptide synthesizer (Applied Biosystems, Foster City, California) starting with Fmoc-Ile-Wang resin. The N-terminus was bromoacetylated using bromoacetic anhydride. The bromoacetylated peptidyl resin was then treated with N-Boc-ethylenediamine. The simultaneous removal of protecting groups and cleavage of the peptide from the resin was carried out in trifluoroacetic acid. Subsequently, trifluoroacetic acid was removed in vacuo, diethyl ether added to the residue, and the precipitated peptide washed with diethyl ether and dried. The crude peptide, fluorescein N-hydroxysuccinimide ester, and N-methylmorpholine were dissolved in dimethylformamide-affording fluorescein APA (Fig. 1A). The reaction

NIH-PA Author Manuscript

NIH-PA Author Manuscript

NIH-PA Author Manuscript

product was purified by preparative reversed-phase high performance liquid chromatography. The pure fluorescein APA was analyzed by analytical high performance liquid chromatography and electrospray mass spectrometry.

Synthesis of chelate-coupled losartan-Leu-Diglycoloyl-PEG(4)-Tetraamine and radiolabeling

The optimal pharmacokinetic profile of an imaging agent differs radically from therapeutic drugs in that rapid excretion from blood is advantageous. Because peptides are particularly better suited for targeting in vivo due to a superior biodistribution profile, we introduced peptide characteristics into the losartan pharmacophore. To facilitate a convenient and rapid synthesis, we adopted a solid phase approach where losartan was immobilized on a trityl resin through its tetrazole group. Further replacement of the hydroxyl group by an amino group enabled attachment of amino acids, linkers, and tetracycline chelates by standard peptide synthesis methods. This strategy did also increase the affinity of losartan for AT type-1 receptors. Structure activity data showed that the introduction of the amino acid leucine and a short linker comprising tetraethylene glycol and diglycolic acid between the losartan moiety and the tetra-amine chelate yielded a losartan analog (Fig. 1B) with superior affinity (K_i = 60 pmol/l) to AT receptors compared with losartan (K_i = 10 nmol/l) and an acceptable biodistribution profile with mainly urinary excretion.

Mouse model of HF

Male Swiss Webster mice (weight 20 to 30 g, Charles River, Wilmington, Massachusetts) were anesthetized with pentobarbital (75 mg/kg by intraperitoneal injection) and intubated with a 21-G tube for mechanical ventilation. The electrocardiogram was monitored continuously, and body temperature was maintained throughout the procedure at 36.5°C. Ventilation was maintained at a 250-μl tidal volume and a respiratory rate of 200 breaths/min (MiniVent HSE-HA, Harvard Apparatus, Holliston, Massachusetts). The heart was exposed through the fourth left intercostal thoracotomy, and the left coronary artery was ligated at its second branching point with a 6-0 Prolene suture. After watching the animal carefully for 30 min, the chest was closed using a 6-0 Monocryl suture. The animals were subjected to optical or radionuclide imaging at various time points in follow-up. Before imaging, anesthetized animals were examined by transthoracic echocardiography using a 14-MHz linear probe (Acuson 15L8, Siemens, Malvern, Pennsylvania). B-mode images of LV parasternal long axis and short axis were obtained and digitally analyzed as described previously (9).

Optical imaging using fluorescent APA

Frozen dried aliquot (100 μg) of the compound was dissolved in 200 μl of distilled water. After cannulation of the internal jugular vein, 50 μg of fluorescent APA was injected. Real-time optical imaging was performed from baseline to 30 min as previously described (10) using a fluorescence stereomicroscope (Leica MZ16FA, Leica Microsystems, Heerbrugg, Switzerland) equipped with a charge-coupled device camera (Orca 285, Hamamatsu, Japan). A 470/50-nm bandpass excitation filter was used, and emitted fluorescence was collected through a bandpass filter of 525/50 nm. Images were analyzed using SimplePCI software (Compix, Sewickley, Pennsylvania). In vivo optical imaging was performed on the day of MI, 30 min after coronary ligation (n = 3); day 1 (n = 3); and weeks 1 (n = 3), 3(n = 3),6(n = 3), and 12 (n = 1) after MI in open-chested mice. Fluorescence APA imaging was also performed in 3 unmanipulated control mice.

Radionuclide imaging using radiolabeled losartan

Radiolabeled losartan was used in 4 mice, 3 weeks after MI and 6 unmanipulated age-matched control mice, using a dual-head micro-SPECT gamma camera and a micro-CT (X-SPECT, Gamma Medica, Northridge, California). The SPECT images were acquired in a 64 × 64

NIH-PA Author Manuscript

NIH-PA Author Manuscript

NIH-PA Author Manuscript

matrix, 32 steps at 20 s (0 h) or 120 s (at 4 h) per step at 140-KeV photopeak of ^{99m}Tc-losartan with a 15% window using a low-energy, high-resolution parallel collimator. The CT images were acquired without moving the animals. The micro-CT uses an X-ray tube operating at 50 kVp and 0.6 mA, with images captured for 2.5 s per view for 256 views in 360° rotation. Micro-CT images were transferred to a 256 × 256 matrix and micro-CT tomographic studies were fused, facilitating scintigraphic and anatomic information in all tomographic scans in 3 spatial axes. Animals were killed by an overdose of pentobarbital (120 mg/kg) after the imaging experiments. Hearts were carefully extracted and planar images of ex vivo heart were acquired for 15 min in a 128 × 128 matrix using a low-energy, high-resolution, pinhole collimator. Thereafter, each heart was cut into 3 bread-loaf slices (infarct, peri-infarct, and remote areas). The quantitative radiolabeled losartan uptake was determined with a gamma scintillation counter (1480 Wizard 3-inch; Wallac Co., Turku, Finland).

Pathologic characterization of the myocardial tissue

Hearts harvested after the optical imaging experiments were used for histopathologic characterization taking advantage of the intravenously administered fluorescent AT receptor probe. For this purpose, half of the myocardial tissue specimens were snap-frozen. Frozen sections (7 μm) of the heart were cut and examined by confocal microscopy (Axioplan 2, Zeiss, Göttingen, Germany) directly without further preparation. Subsequently, the same myocardial tissue specimens were stained with α-smooth muscle actin (SMA) antibody (Sigma, St. Louis, Missouri) for localization of myofibroblasts. The antibody for SMA was conjugated to a rhodamine-linked secondary antibody. Individual localization of APA and SMA were registered and merged subsequently to investigate colocalization. To further characterize cellular APA uptake, the infarcted myocardial region was also analyzed by 2-photon microscopy. This imaging setup consisted of a mode-locked Ti:Sapphire laser (170-fs pulse width, 76 MHz repetition rate; Mira 900F, Coherent Radiation, Palo Alto, California) pumped by a 5-W Verdi laser (Coherent Radiation). The 800-nm wavelength excitation beam was deflected into the back port of an inverted Axiovert 100 microscope (Zeiss) and scanned across the sample by a personal computer– controlled galvanometer-driven *x-y* scanner (Series 603X, Cambridge Technology, Watertown, Massachusetts). The beam was then reflected by a short-pass 675-nm dichroic beam splitter (Chroma Technology, Brattleboro, Vermont) and focused onto the sample with a 63×, water-immersion microscope objective (C-Apochromat, numerical aperture = 1.2, Zeiss). The average excitation power entering the microscope was approximately P = 60 mW (corresponding to 5 mW at the sample site). The fluorescence and second harmonic generation signals from the sample were discriminated by a 675-nm short-pass dichroic mirror, transmitted through a short-pass 600-nm filter (CVI Laser, Livermore, California), and further split by secondary long-pass 510-nm dichroic mirror onto 2 photomultiplier tubes with narrow (10-nm bandwidth) bandpass 400-nm filter (Chroma Technology) for second harmonic generation collection and 535-nm (50-nm bandwidth) band-center filter (Chroma Technology) for green fluorescence collection. Images (256 × 256 pixels) were taken at various depths (z), covering an area of 35 × 35 μm^2 for the 63× microscope objective. Each acquisition was integrated for 10 s. The remaining half of the myocardial tissue specimens were fixed with 4% phosphate-buffered paraformaldehyde; fixed myocardial tissue specimens were analyzed routinely by hematoxylin and eosin staining.

Statistical analysis

All quantitative results are presented as the mean ± SD. To determine statistical significance of differences, Mann-Whitney test was used and a p value smaller than 0.05 was considered significant.

NIH-PA Author Manuscript

NIH-PA Author Manuscript

NIH-PA Author Manuscript

RESULTS

Real-time optical imaging of myocardial angiotensin receptors in HF

Optical imaging was performed with fluoresceinated APA. Although all infarcts were non-reperfused, the tracer entry in the infarcted myocardium occurred within 3 min and maximized in 20 min (Figs. 2A to 2D). In addition to myocardial localization, coronary arteries and arterioles showed intense uptake of the ligand; the uptake was minimal in the venous tree (Fig. 2E). No uptake of fluorescent APA probe was observed in the infarct area immediately after MI and 1 day after MI. However, distinct APA uptake was observed in the infarct regions at 1 week following MI, which increased substantially by 3 weeks (Fig. 3A). Minimal uptake of fluorescent probe was observed in the remote areas. Subsequently, the uptake in infarct region decreased at 6 weeks after MI and was predominantly seen in the infarct border zone (Fig. 2D). Uptake resolved by the 12th week. Echocardiographic examination demonstrated left ventricular dilation over time indicating progressive cardiac remodeling (Fig. 3B). Unmanipulated control animals receiving fluorescent APA did not show tracer uptake (Fig. 3A).

Pathologic characterization of receptor targeting

Direct localization of systemically administered fluorescent APA probe allowed characterization of binding sites of AT receptors in the myocardial tissue specimens. The APA uptake (green, Figs. 4A and 4B) was almost exclusively localized in cells other than cardiomyocytes. The fluorescently labeled cells in the replacement fibrosis in infarcted and peri-infarcted regions (green, Fig. 4D) stained positively for α-SMA (red, Fig. 4E). These data suggest that binding of the APA occurs, at least in a large part, to myofibroblasts (yellow, Figs. 4D to 4F). Although no uptake was seen in the cardiomyocytes, endothelial cells, or interstitial cells, APA uptake was distinctly observed in the vascular medial layers in arterioles. Two-photon microscopy revealed internalization of the green APA probe within the myofibroblasts and demonstrated intracellular and nuclear localization of the APA (Fig. 4C). Using second harmonic generation imaging, collagen fibers (blue) were seen emanating from the APA-positive cells, which further suggests the myofibroblastic origin of these cells (Fig. 4C).

Nuclear imaging of angiotensin receptors

For noninvasive imaging of angiotensin receptors, we used radiolabeled losartan, in the 3-week post-MI animals for micro-SPECT/micro-CT imaging; a 3-week post-MI model was chosen for radionuclide imaging because of maximal upregulation of AT receptors observed in the optical imaging experiments. Radiolabeled losartan uptake was compared with unmanipulated control animals (Fig. 5). The combination of micro-SPECT and -CT images allowed for precise localization of myocardial uptake, which was observed in the anterolateral cardiac region. Ex vivo imaging of the explanted hearts demonstrated uptake in the infarct and border territory (Fig. 5C). Quantitative radiotracer uptake in infarcted myocardium, represented as percentage of injected radiotracer uptake per gram of myocardial tissue, was significantly higher than in control hearts ($0.52 \pm 0.21\%$ vs. $0.21 \pm 0.13\%$, $p < 0.05$). The mean infarct-to-remote region uptake ratio was 2.4:1. The maximum non-target organ radiation burden was observed in liver and kidney.

DISCUSSION

The pivotal role of the renin-angiotensin system in ventricular remodeling following MI has been established in numerous experimental and clinical studies. More than circulating renin-angiotensin levels, it is the myocardial upregulation of ACE, AT and its receptors, which determine the likelihood of ventricular remodeling (3,11). As such, the use of angiotensin receptor blockers (6,12) and ACE inhibitors (13–15) has resulted in improved survival in

NIH-PA Author Manuscript

NIH-PA Author Manuscript

NIH-PA Author Manuscript

patients with manifest and subclinical HF. It has been suggested that maximization of anti-angiotensin therapy, including increase in ACE-inhibitor dose or addition of angiotensin receptor blockers over ACE-inhibitor therapy further reduces morbidity (6,16) and mortality (4) in HF. It is therefore conceivable that accurate assessment of myocardial AT receptor expression should guide optimization of anti-angiotensin therapy. It should also allow periodic evaluation of the efficacy of anti-angiotensin intervention. Current diagnostic imaging of HF remains generally focused on geometric and structural cardiac alterations (17,18), and it can be hypothesized that the ability to visualize interstitial processes at the molecular level, which precede the geometric and functional deterioration of the left ventricle, should help predict the likelihood and rate of remodeling and development of HF (19).

The present study demonstrates the feasibility of in vivo imaging of myocardial angiotensin receptors in an experimental HF model. Currently, as a strategy for prevention of advanced HF, significant emphasis is being placed on the recognition of patients at risk for developing HF, including those with no apparent structural LV abnormality (stage A) and asymptomatic patients with a known structural LV abnormality (stage B) (20). As the current clinical practice allows diagnosis of HF only after the LV has undergone substantial remodeling, development of a technology that actually predicts occurrence of cardiac remodeling is of critical importance. Our immunohistochemical analyses show that binding of the tracer uptake was almost exclusively localized to myofibroblasts; we did not observe APA uptake in cardiomyocytes. Upregulation of AT receptors on myofibroblasts (Fig. 4F) allows for growth factor (such as AT)–induced myofibroblast proliferation and collagen production, which is believed to contribute to healing and the remodeling process following MI (2,21,22). Although angiotensin receptor upregulation in the kidneys has been observed earlier by a carbon-11 labeled AT type-1 antagonist (23), the hypothesis of the role of targeting neurohumoral upregulation for ventricular remodeling has been supported by imaging of renin-angiotensin axis with the help of radiolabeled benzoyl lisinopril (21,24). Dilsizian et al. (24) incubated myocardial specimens explanted from patients undergoing cardiac transplantation for end-stage ischemic cardiomyopathy with F-18 fluoro-benzoyl lisinopril. There was specific binding of radiotracer to ACE; mean binding was 6.6 ± 5.2, compared with 3.4 ± 2.5 luminescence/mm^2 in segments pre-incubated with cold lisinopril ($p < 0.0001$). Further, mean radiotracer binding was 6.3 ± 4.5 in infarcted, 7.6 ± 4.7 in peri-infarcted, and 5.0 ± 1.0 luminescence/mm^2 in remote non-infarcted ($p < 0.02$) segments. The distribution of mast cell chymase was nonuniform in these samples and disparate from ACE. This and the study presented here demonstrate that ACE (and probably AT) upregulation induces the proliferation of myofibroblasts (which have increased angiotensin receptor density) and contributes to collagen deposition. Both studies have also demonstrated that these key steps in the tissue renin-angiotensin cascade involve receptor upregulation of only about 2- to 3-fold. It therefore remains to be seen whether imaging targeted to AT receptors and/or ACE will result in clinically robust imaging strategy.

CONCLUSIONS

The present study explains the development of a diagnostic probe seeking AT receptor upregulation within the myocardium and shows the feasibility of noninvasive radionuclide imaging. The fluorescent angiotensin receptor probe confirms receptor localization on myofibroblasts, which may contribute to the process of interstitial fibrosis. It is proposed that monitoring of angiotensin receptor expression after infarction may predict the evolution of HF. The present study offers a proof of concept, with modest uptake of radiolabeled losartan and it will be necessary to engineer probes with better targeting characteristics for realization of potential clinical application.

NIH-PA Author Manuscript

NIH-PA Author Manuscript

NIH-PA Author Manuscript

Acknowledgments

Supported in part by GE Healthcare (Oslo, Norway) that provided the fluorescent and radiolabeled probes for imaging; the Laser Microbeam and Medical Program (LAMMP) and NIH Biomedical Technology Resource grant #P41-RR01192, both of which supported the optical imaging and analysis; and by DiPalma-Brodsky funds that provided research fellowship support to Dr. Verjans. Drs. Lovhaug, B. Indrevoll, Dr. Bjurgert, L. Peterson, Dr. Kindberg, Dr. Solbakken, and Dr. Cuthbertson are employees of GE Healthcare, Oslo, Norway. H. William Strauss, MD, acted as Guest Editor for this paper.

ABBREVIATIONS AND ACRONYMS

ACE	angiotensin-converting enzyme
APA	angiotensin peptide analog
AT	angiotensin II
CT	computed tomography
HF	heart failure
LV	left ventricle
MI	myocardial infarction
SMA	smooth muscle actin
SPECT	single-photon emission computed tomography

REFERENCES

1. Paul M, Poyan Mehr A, Kreutz R. Physiology of local renin-angiotensin systems. Physiol Rev 2006;86:747–803. [PubMed: 16816138]
2. Weber KT. Extracellular matrix remodeling in heart failure: a role for de novo angiotensin II generation. Circulation 1997;96:4065–82. [PubMed: 9403633]
3. Harada K, Sugaya T, Murakami K, Yazaki Y, Komuro I. Angiotensin II type 1A receptor knockout mice display less left ventricular remodeling and improved survival after myocardial infarction. Circulation 1999;100:2093–9. [PubMed: 10562266]
4. Pfeffer MA, Swedberg K, Granger CB, et al. Effects of candesartan on mortality and morbidity in patients with chronic heart failure: the CHARM-Overall programme. Lancet 2003;362:759–66. [PubMed: 13678868]
5. Pitt B, Poole-Wilson PA, Segal R, et al. Effect of losartan compared with captopril on mortality in patients with symptomatic heart failure: randomised trial—the Losartan Heart Failure Survival Study ELITE II. Lancet 2000;355:1582–7. [PubMed: 10821361]
6. Cohn JN, Tognoni G. A randomized trial of the angiotensin-receptor blocker valsartan in chronic heart failure. N Engl J Med 2001;345:1667–75. [PubMed: 11759645]
7. The CONSENSUS Trial Study Group. Effects of enalapril on mortality in severe congestive heart failure. Results of the Cooperative North Scandinavian Enalapril Survival Study (CONSENSUS). N Engl J Med 1987;316:1429–35. [PubMed: 2883575]
8. The SOLVD Investigators. Effect of enalapril on survival in patients with reduced left ventricular ejection fractions and congestive heart failure. N Engl J Med 1991;325:293–302. [PubMed: 2057034]
9. Kocher AA, Schuster MD, Szabolcs MJ, et al. Neovascularization of ischemic myocardium by human bone-marrow-derived angioblasts prevents cardiomyocyte apoptosis, reduces remodeling and improves cardiac function. Nat Med 2001;7:430–6. [PubMed: 11283669]
10. Dumont EA, Reutelingsperger CP, Smits JF, et al. Real-time imaging of apoptotic cell-membrane changes at the single-cell level in the beating murine heart. Nat Med 2001;7:1352–5. [PubMed: 11726977]

NIH-PA Author Manuscript

NIH-PA Author Manuscript

NIH-PA Author Manuscript

11. Lamas GA, Pfeffer MA. Left ventricular remodeling after acute myocardial infarction: clinical course and beneficial effects of angiotensin-converting enzyme inhibition. Am Heart J 1991;121:1194–202. [PubMed: 1826184]
12. Dickstein K, Kjekshus J. Effects of losartan and captopril on mortality and morbidity in high-risk patients after acute myocardial infarction: the OPTIMAAL randomised trial. Optimal Trial in Myocardial Infarction with Angiotensin II Antagonist Losartan. Lancet 2002;360:752–60. [PubMed: 12241832]
13. The Acute Infarction Ramipril Efficacy (AIRE) Study Investigators. Effect of ramipril on mortality and morbidity of survivors of acute myocardial infarction with clinical evidence of heart failure. Lancet 1993;342:821–8. [PubMed: 8104270]
14. Pfeffer MA, Braunwald E, Moye LA, et al. Effect of captopril on mortality and morbidity in patients with left ventricular dysfunction after myocardial infarction. Results of the survival and ventricular enlargement trial. The SAVE Investigators. N Engl J Med 1992;327:669–77. [PubMed: 1386652]
15. Kober L, Torp-Pedersen C, Carlsen JE, et al. A clinical trial of the angiotensin-converting-enzyme inhibitor trandolapril in patients with left ventricular dysfunction after myocardial infarction. Trandolapril Cardiac Evaluation (TRACE) Study Group. N Engl J Med 1995;333:1670–6. [PubMed: 7477219]
16. Packer M, Poole-Wilson PA, Armstrong PW, et al. Comparative effects of low and high doses of the angiotensin-converting enzyme inhibitor, lisinopril, on morbidity and mortality in chronic heart failure. ATLAS Study Group. Circulation 1999;100:2312–8. [PubMed: 10587334]
17. Narula J, Acio ER, Narula N, et al. Annexin-V imaging for noninvasive detection of cardiac allograft rejection. Nat Med 2001;7:1347–52. [PubMed: 11726976]
18. Narula J, Khaw BA, Dec GW Jr. et al. Brief report: recognition of acute myocarditis masquerading as acute myocardial infarction. N Engl J Med 1993;328:100–4. [PubMed: 8416421]
19. Chandrashekhar Y, Narula J. Exposing ACE up the sleeve. J Nucl Med 2007;48:173–4. [PubMed: 17268010]
20. Hunt SA. ACC/AHA 2005 guideline update for the diagnosis and management of chronic heart failure in the adult: a report of the American College of Cardiology/American Heart Association Task Force on Practice Guidelines (Writing Committee to Update the 2001 Guidelines for the Evaluation and Management of Heart Failure). J Am Coll Cardiol 2005;46:e1–82. [PubMed: 16168273]
21. Shirani J, Narula J, Eckelman WC, Narula N, Dilsizian V. Early imaging in heart failure: exploring novel molecular targets. J Nucl Cardiol 2007;14:100–10. [PubMed: 17276312]
22. Weber KT, Brilla CG. Pathological hypertrophy and cardiac interstitium. Fibrosis and renin-angiotensin-aldosterone system. Circulation 1991;83:1849–65. [PubMed: 1828192]
23. Szabo Z, Speth RC, Brown PR, et al. Use of positron emission tomography to study AT1 receptor regulation in vivo. J Am Soc Nephrol 2001;12:1350–8. [PubMed: 11423564]
24. Dilsizian V, Eckelman WC, Loredo ML, Jagoda EM, Shirani J. Evidence for tissue angiotensin-converting enzyme in explanted hearts of ischemic cardiomyopathy using targeted radio-tracer technique. J Nucl Med 2007;48:182–7. [PubMed: 17268012]

NIH-PA Author Manuscript
NIH-PA Author Manuscript
NIH-PA Author Manuscript

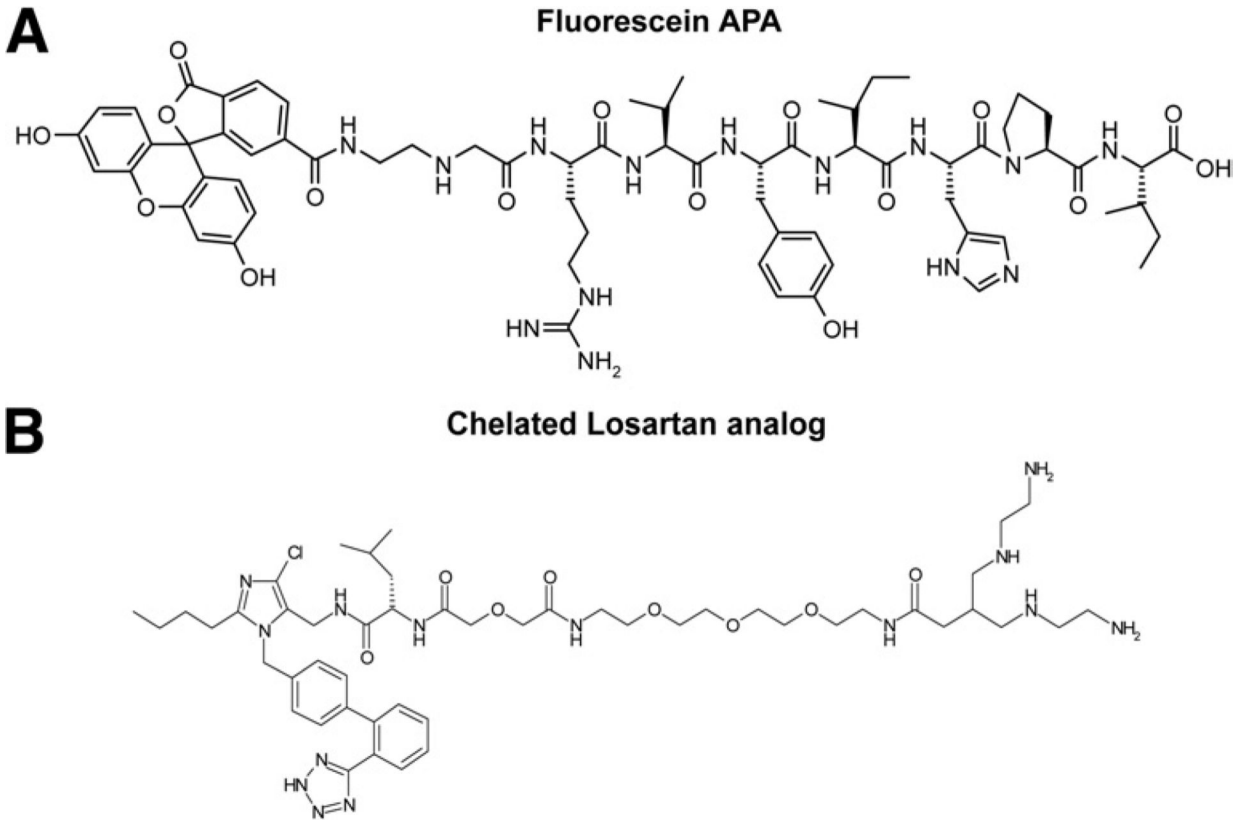

Figure 1. Structure of Tracers Used for AT Receptor Targeting

Fluorescent angiotensin peptide analog (APA) (**A**), technetium Tc-99m losartan (**B**). AT = angiotensin II.

NIH-PA Author Manuscript
NIH-PA Author Manuscript
NIH-PA Author Manuscript

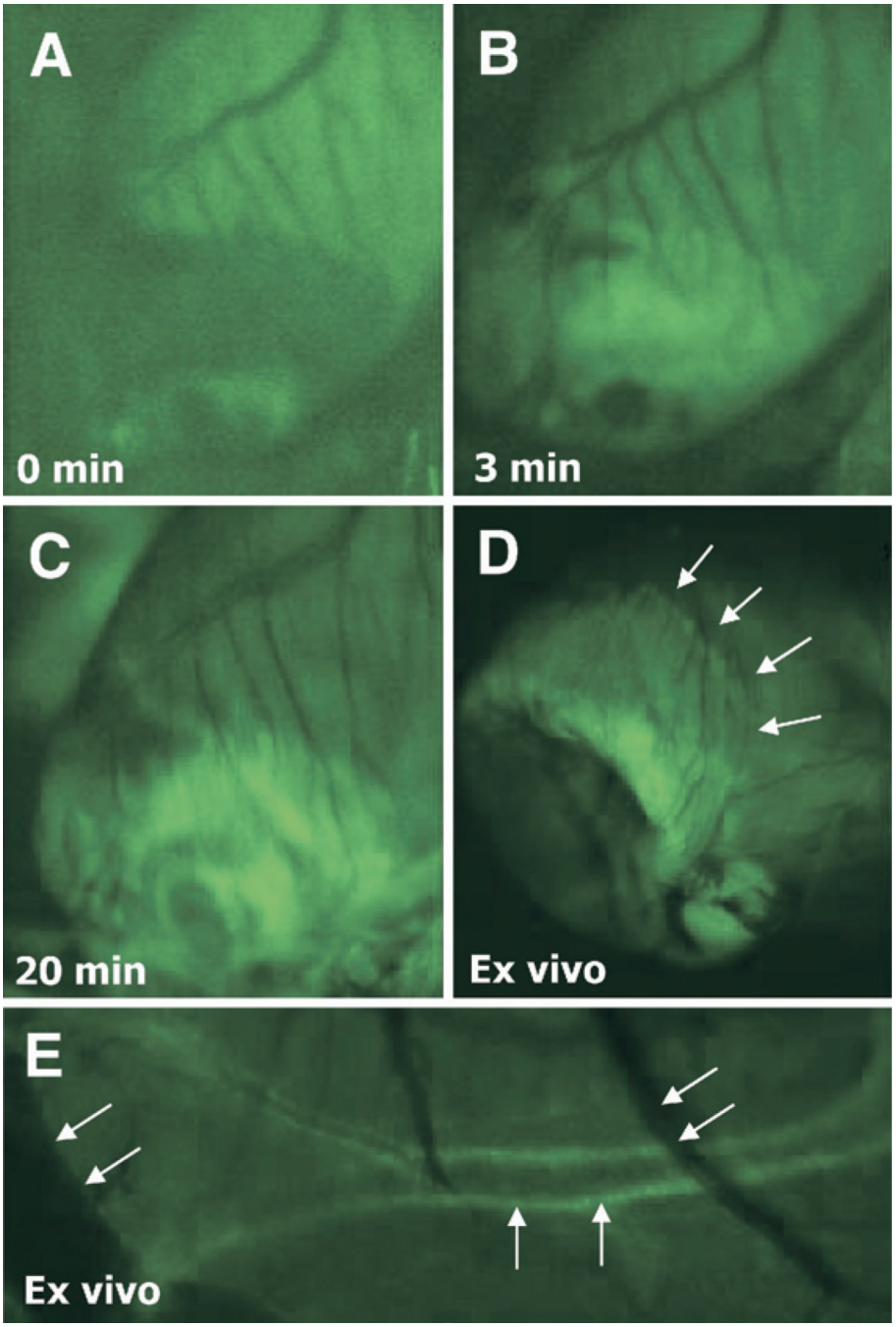

Figure 2. Optical Imaging of AT Receptors

Intravital microscopy images show a 3-week old MI in the murine heart failure model from baseline **(A)**, and 3 min **(B)**, and at 20 min **(C)** after administration of **green** fluorescent angiotensin peptide analog (APA), demonstrating gradual increase of the fluorescent APA in infarcted region. Fluorescent uptake was maximized at 20 min after intravenous APA injection. The ex vivo image **(D)**, demonstrates APA uptake in the border zone, as thinned out infarct zone has collapsed and is therefore not visible. **Panel E** shows APA uptake in smooth muscle cell layer of a small coronary artery **(vertical arrows)** as well as minimal uptake in thinner veins **(diagonal arrows)**

NIH-PA Author Manuscript
NIH-PA Author Manuscript
NIH-PA Author Manuscript

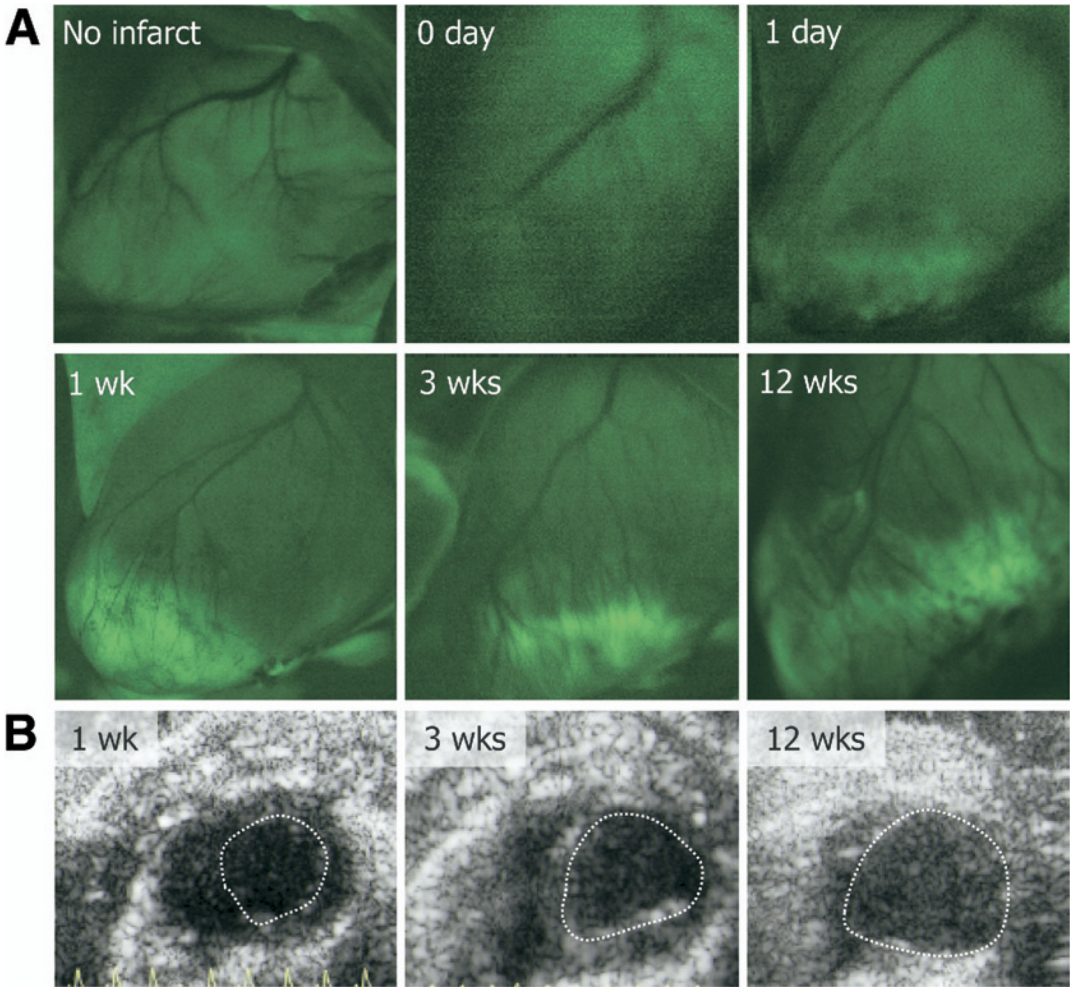

Figure 3. Evolution of APA Uptake After MI

Intravital microscopy images demonstrating uptake of fluorescent APA from 6 groups: no infarction, and 0 day, 1 day, 1 week, 3 weeks and 12 weeks after MI **(A)** The uptake increases from 1 to 3 weeks, and decreases thereafter. **Panel B** shows the respective echocardio-grams at 1, 3, and 12 weeks, indicating left ventricular dilation and progressive heart failure in these mice with MI.

NIH-PA Author Manuscript
NIH-PA Author Manuscript
NIH-PA Author Manuscript

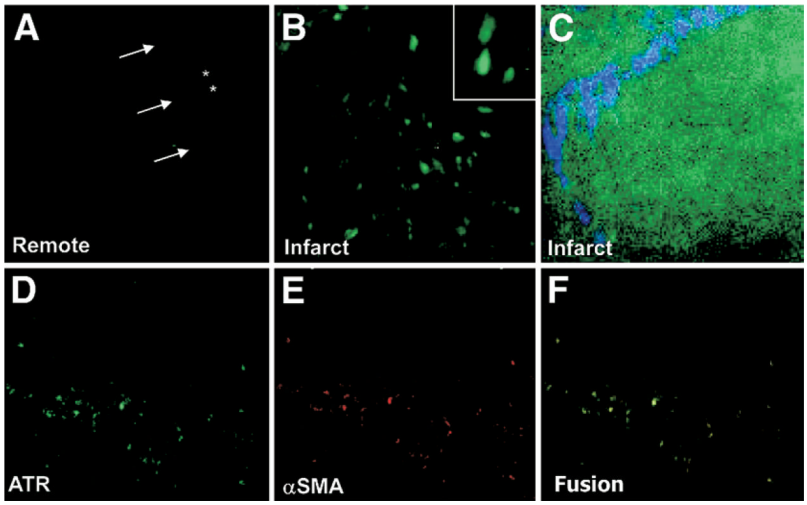

Figure 4. Pathologic Characterization APA Localization

The remote zone **(A)** demonstrates no APA uptake in interstitium **(*)** or cardiomyocytes **(arrows)** The cells of nonmyocytic origin demonstrate fluorescent APA uptake in the infarct zone **(B)**, with an enlarged image of cellular uptake **(inset)** These cells in the infarct region **(D, green)** also stained positively for smooth muscle actin (SMA) **(E, red)**, showing colocalization **(F, yellow)**, indicating AT receptors (ATR) on myofibroblasts. **(C)** Ex vivo 2-photon microscopy demonstrated fluorescent APA intracellularly within the myofibroblast **(green)**, with collagen surrounding the myofibroblast using second harmonic generation imaging **(blue)** Abbreviations as in Figure 1.

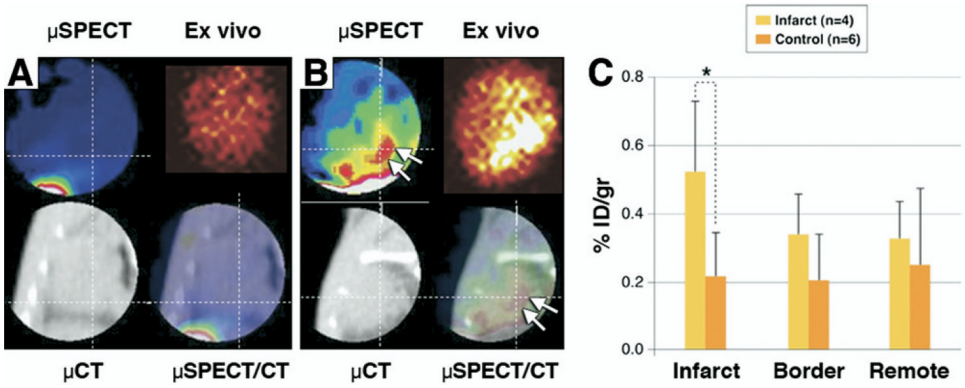

Figure 5. Noninvasive Imaging of AT Receptors With Radiolabeled Losartan

The micro–SPECT and micro-CT images are shown in a control mouse after technetium Tc-99m losartan administration; no uptake in the heart can be seen **(A)** in the in vivo and ex vivo images. There is only some liver uptake on the **bottom left** of the SPECT image. **(B)** In the 3-week post-MI animal, significant radiolabeled losartan uptake is observed in the anterolateral wall **(arrows)** The infarct uptake on the in vivo image is confirmed in the ex vivo image. The histogram **(C)** demonstrates significantly (*) higher uptake in the infarcted region (0.524 ± 0.212% ID/g) as compared to control noninfarcted animals (0.215 ± 0.129% ID/g; $p < 0.05$). ID = injected dose.

NIH-PA Author Manuscript
NIH-PA Author Manuscript
NIH-PA Author Manuscript

NIH-PA Author Manuscript
NIH-PA Author Manuscript
NIH-PA Author Manuscript

Table 1

Optical and Nuclear Imaging Groups and Timeline of Imaging

			Post-MI Mice						
Tracer	**Probe**	**Control Mice**	**0 days**	**1 day**	**1 week**	**3 weeks**	**6 weeks**	**12 weeks**	**Total**
GFP	APA	3	3	3	3	3	3	1	19
^{99m}Tc	Losartan	6				4			10

APA = angiotensin peptide analog; GFP = green fluorescent protein; MI = myocardial infarction; ^{99m}Tc = technetium-99m.